Contributed Papers from Materials Science and Technology 2019 (MS&T19)
September 29–October 3, 2019, Oregon Convention Center, Portland, Oregon, USA

DOI 10.7449/2019/MST_2019_1208_1216

PREPARATION OF Mo_2C BY REDUCTION AND CARBONIZATION OF MoO_2 WITH ETHANOL

Zepeng Lv[1], Jie Dang[1,*], Chenguang Bai[1]

[1]College of Materials Science and Engineering, Chongqing University; Chongqing 400044, PR China

Keywords: MoO_2, ethanol, Mo_2C, reduction, carbonization

Abstract

Molybdenum hemicarbide (Mo_2C) can be widely used in steel, metal ceramics and catalyst of hydrogen involved reactions. This work reported a simple method for preparing molybdenum hemicarbide by reducing and carbonizing MoO_2 with ethanol. Thermodynamic analysis was performed to predict experimental conditions for Mo_2C formation in the MoO_2-C_2H_5OH-Ar system with Ar/C_2H_5OH molar ratio of 6.82 (Ar was used as a carrier gas for ethanol). XRD and SEM analyses were carried out for phases' and morphological studies. Based on the results, the reaction and carbonization routes were obtained: MoO_2 was reduced and carburized directly to Mo_2C in one step at lower temperatures, and first reduced to metallic Mo and then carburized to Mo_2C at higher temperatures. The reduction mechanisms were proposed: the pseudomorphic transformation mechanism dominated the reaction at low temperatures, but at high temperatures, the reaction obeyed the chemical vapor transport (CVT) mechanism.

1. Introduction

Transition metal carbides, a new type of functional material, possess a good development potential and have received a lot of attention. Those carbides have a wide range of applications because of their advantages, such as high melting point, high hardness, high elastic modulus, good heat and electrical conductivity and excellent corrosion resistance. For another, improving the performance of materials with the addition of metal carbides is also an important application, such as increasing the high temperature resistance, abrasion and chemical corrosion resistances [1,2]. Mo_2C (Molybdenum hemicarbide) has not only the characteristics of metal carbides, but also the catalytic properties, and it could be widely used as the catalyst of hydrogen involved reactions, such as hydrogenation desulfurization, unsaturated hydrocarbon hydrogenation, isomerization, denitrification reaction [3-5] and hydrogenation deoxygenation [6]. The production of Mo_2C has attracted much attention in recent years and a number of methods of preparation Mo_2C have been developed. The proposed methods mainly include: gas reduction [7-12], sonochemical synthesis [13], alkalide reduction [14], a solution derived precursor method [15,16] and high-energy ball milling [17]. Although molybdenum carbides (Mo_2C or MoC) can

*Corresponding author: Jie Dang
E-mail: jiedang@cqu.edu.cn; Phone: +86-23-65112631; Fax: +86-23-65112631
Address: College of Materials Science and Engineering, Chongqing University, Chongqing 400044, PR China

be synthesized successfully through these methods, there are still some defects, such as the complexity of technological process, a higher temperature and a long time.

In the present work, the liquid ethanol (C_2H_5OH) was chosen as a reducing and carbonizing source with the advantages of renewable, cheap, high in hydrogen content, safe to handle and transport, biodegradable, increasingly available and it can be produced in large quantities from various sources (biomass, plants and wasted materials). Hence, the present work aims to research the pyrometallurgical reduction and carbonization of MoO_2 with C_2H_5OH to prepare Mo_2C. The theoretical calculation of the MoO_2-C_2H_5OH-Ar system was also carried out to predict and help to understand the formation mechanism of Mo_2C.

2. Materials and Experimental

2.1 Materials

Commercially available MoO_2 powders (Jinduicheng Molybdenum Co., Ltd) were used as the experimental raw material. The Scanning Electron Microscope (SEM) image of raw MoO_2 is shown in Figure 1 and it can be clearly seen that the powder is composed of many small platelet-shaped particles. The particle size distribution of MoO_2 was measured with a laser interferometer (LMS-30; Seishin Enterprise Co., Ltd., Tokyo, Japan), as reported elsewhere [18], giving an average particle size of 14.4 μm.

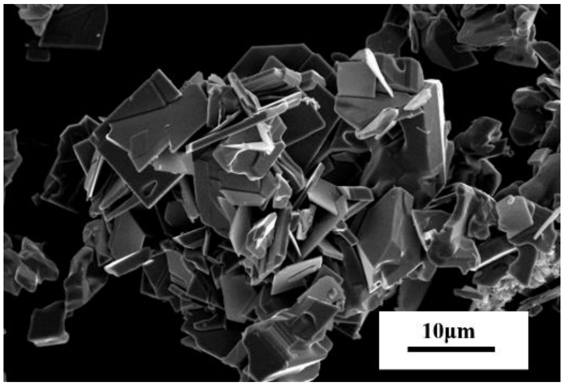

Figure 1. The SEM image of raw MoO_2 powder.

2.2 Experimental

To monitor the weight change of samples during the reduction continuously, a thermo-gravimetric analyzer (HCT-3, Beijing Hengjiu, Instrument Ltd., China) was used, and the corresponding schematic diagram of the experimental device is shown in Figure 2. A sample of around 100 mg was used in each experimental run and after an alumina crucible (8×8mm) with samples was put into the TGA, high-purity argon was introduced to flush air out of the furnace through route 1. In isothermal reduction, the furnace was first heated from room temperature up to the different desired temperatures with the ramping rate of 10K/min in pure Ar. After an equilibration time of 20 min to stabilize sample's temperature, ethanol which was carried by argon gas (the liquid ethanol bath kept in a bubbler at 303K) was introduced into the furnace through route 2. After reacting for a certain time, the reaction gas was switched to pure argon again, and samples were cooled down to room temperature. Non-isothermal experiments were carried out from room temperature to 1423K with three ramping rates, namely, 3, 6, and 9 K/min.

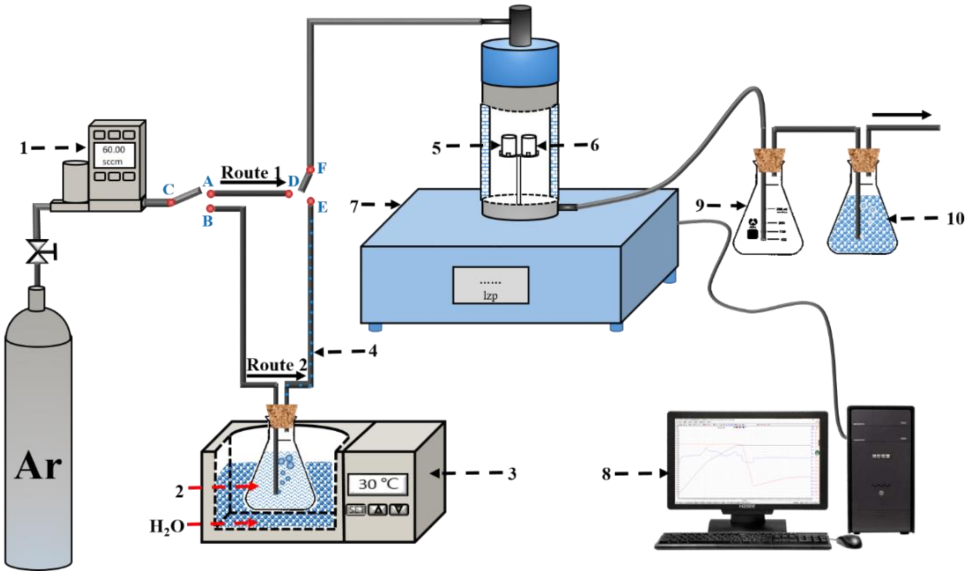

Figure 2. Schematic diagram of the experimental apparatus for the TG analysis. 1-Gas flow controller, 2-Ethanol solution, 3-Water bath, 4-Ethanol vapor, 5-Calibrated alumina crucible, 6-Experimental alumina crucible, 7-HCT-3 TG analyzer, 8-Data collector, 9-Beaker flask A, 10-Beaker flask B.

In all experiments, the flow rate of argon gas was kept a constant value of 60 sccm (standard cm^3/min). The flow rate of gaseous ethanol (F^o_{ethanol}) carried by Ar was calculated by the following formula [19,20]:

$$F^o_{\text{ethanol}} = \frac{F^o_{Argon} P_{ethanol}}{P_{total} - P_{ethanol}} \tag{1}$$

where F^o_{Argon}, P_{total}, and $P_{ethanol}$ were flow rate of the carrier gas Ar. All the experiments were done at a constant Ar/C_2H_5OH molar ratio of 6.82.

The flow rate of gas was controlled by gas flow controllers (Alicant, Model MC-500SCCM-D). X-Ray Diffraction (XRD) (PANalytical X'Pert Powder, Panalytical B.V.) measurements were conducted for the reacted samples. Morphologies of these samples were observed using SEM (TESCAN VEGA 3 LMH, Czech Republic) technique. Thermodynamic calculations were performed by using FactSage 6.2 with pure substances database.

3. Thermodynamic Analysis

In this work, C_2H_5OH and MoO_2 were used as reactants, and C_2H_5OH vapor was carried into the reaction system with Ar as the carrier. To conduct the expected reactions, the equilibrium calculation was carried out in the Mo-C-O-H system in the temperature range of 1000-1500K at a pressure of 1 atm with an Ar/C_2H_5OH molar ratio of 6.82, which is experimentally attainable. In the system, 50 species of gas phase components (mainly included H_2, CO, $H_2O(g)$, CO_2, CH_4, CH_3, $MoO_2(OH)_2$, C_2H_4, H_2CO, H) were considered, and the condensed equilibrium phases were C, MoO_2, Mo and Mo_2C. Figure 3 shows the solid phase fields computed as a function of temperature and the input C_2H_5OH mole fraction (X_{C2H5OH}) which is given by $n^o_{C2H5OH}/(n^o_{C2H5OH}+n^o_{MoO2})$ where n^o_{C2H5OH}, n^o_{MoO2} stand for the input numbers of moles of the ethanol and MoO_2, respectively. As shown in the figure, Mo begins to be formed above 1220K and when the temperature rises up to 1235K, MoO_2 is first reduced to Mo, and single Mo phase field further enlarges as the temperature increases. It suggests that the reduction follows the path of $MoO_2 \rightarrow Mo \rightarrow Mo_2C$ when temperature is over 1235K; but at the temperature blow 1220K, MoO_2 reacts with ethanol to form Mo_2C directly, without forming metallic Mo, and thus the reduction follows the path of $MoO_2 \rightarrow Mo_2C$.

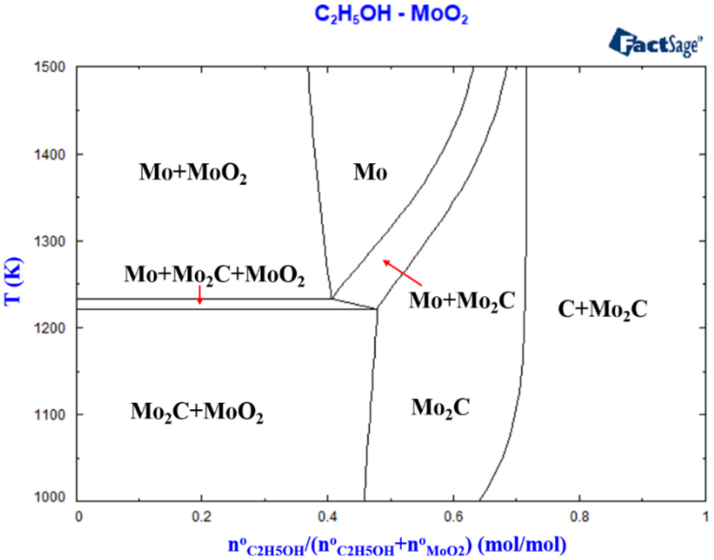

Figure 3. Equilibrium diagram showing solid phase fields as a function of temperature and input ethanol mole fraction in the MoO_2-C_2H_5OH system.

4.Results and Discussion

4.1 Non-Isothermal Reaction

In order to clarify the reaction initial temperature and the effect of ramping rates on the reaction, non-isothermal reduction of MoO_2 powders with C_2H_5OH vapor was performed at three different ramping rates, 3, 6, and 9 K/min. The reduction curves (Figure 4(a)) show that all mass changes started at around 1073K (800^{o}C) and were complete at a temperature of below 1423K (1150^{o}C). The weight change increased smoothly to around -20.32% (corresponding to the theoretical weight change from MoO_2 to Mo_2C). X-ray diffraction, shown in Figure 5, confirmed that the final product was pure Mo_2C. According to the curves shown in Figure 4(b), it can be proved that a higher heating rate caused a faster the reaction rate. There is only one peak in the DTG (differential thermogravimetry) curve of 3K/min but two peaks in the curves of 6 and 9K/min, indicating that only loss-mass reaction occurred with the ramping rate of 3K/min, and Mo_2C was formed by reduction and carburization in one step. While when the ramping rate is over 6K/min, the reaction curve first went to a value between -20.32% (corresponding to forming Mo_2C) and -25.01% (corresponding to forming Mo), and then returned to -20.32%. It indicated that only part of MoO_2 was reacted follow the path of $MoO_2 \rightarrow Mo \rightarrow Mo_2C$. The reason was that

Mo_2C was formed directly at lower temperatures, but with increasing the temperature, metallic Mo would be formed first (increase of the ramping rate resulted in rapid approaching the temperature of Mo formation). When the ramping rate was 9K/min, the weight loss ratio first increased up to 25.01%, and finally decreased to 20.32%.

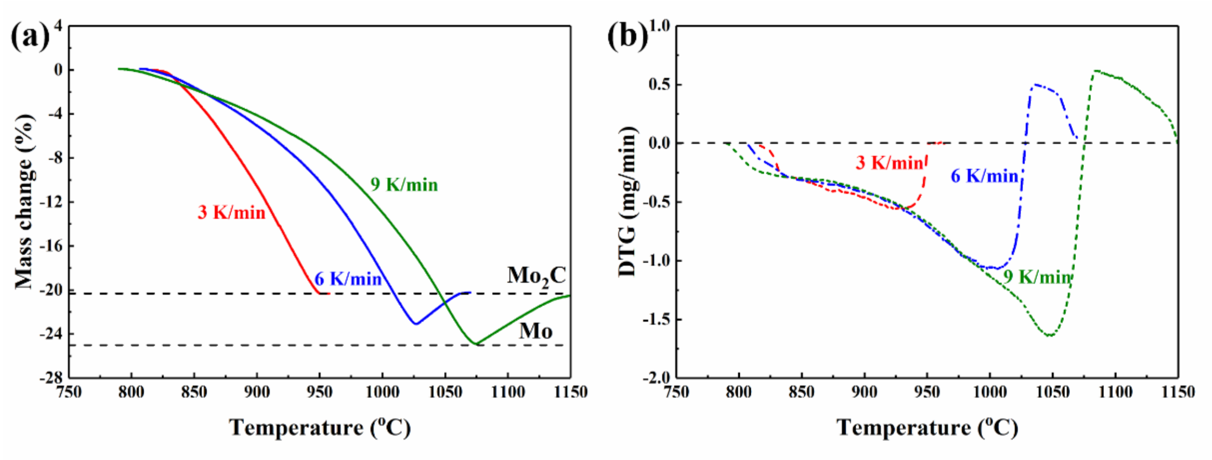

Figure 4. Non-isothermal reduction curves of MoO_2 with C_2H_5OH vapor: (a) weight change verse time, (b) DTG versus temperature.

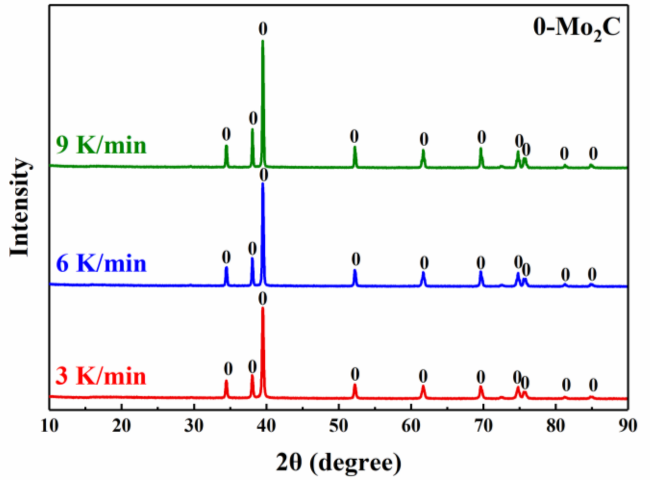

Figure 5. XRD patterns of the non-isothermal products of MoO_2 by C_2H_5OH vapor at different ramping rates. (equipped with a Cu tube)

4.3 Isothermal reaction

The isothermal reduction curves of MoO_2 powders by C_2H_5OH vapor are shown in Figure 6(a) which includes four different temperatures (1134K to 1351K). At lower temperatures (1134-1187K), the mass loss increased smoothly to around 20.32% in one step. While at the moderate temperature of 1253K, the nadir point existed in the curve was between -20.32% and -25.01% which illustrated that partly MoO_2 was involved in the reduction $MoO_2 \rightarrow Mo$. However, the weight loss ratio, at higher temperatures (1351K), first increased up to 25.01%, then decreased to 20.32% in the end. XRD analyses are shown in Figure 6(b) which confirms that the final products were all Mo_2C whether reactions occurred at low temperatures or high temperatures. This reaction behavior is consistent with the expected reaction sequence: at lower temperatures, reduction and carburization occur simultaneously to form Mo_2C directly from MoO_2; whereas at higher temperatures, two steps are expected (reduction in MoO_2 to Mo, followed by carburization of Mo to form Mo_2C). At lower temperatures, the reaction rate increased with temperature increasing. While at high temperatures, the first reduction step and the carbonization step were changed with a contrary tendency. With the increase of temperature, the reaction rate increased as well, but the carbonization rate decreased. According to the equilibrium diagram shown in Figure 3, the theoretical ethanol partial pressure required for the carbonization process is much higher and the carbonization becomes difficult at high temperatures.

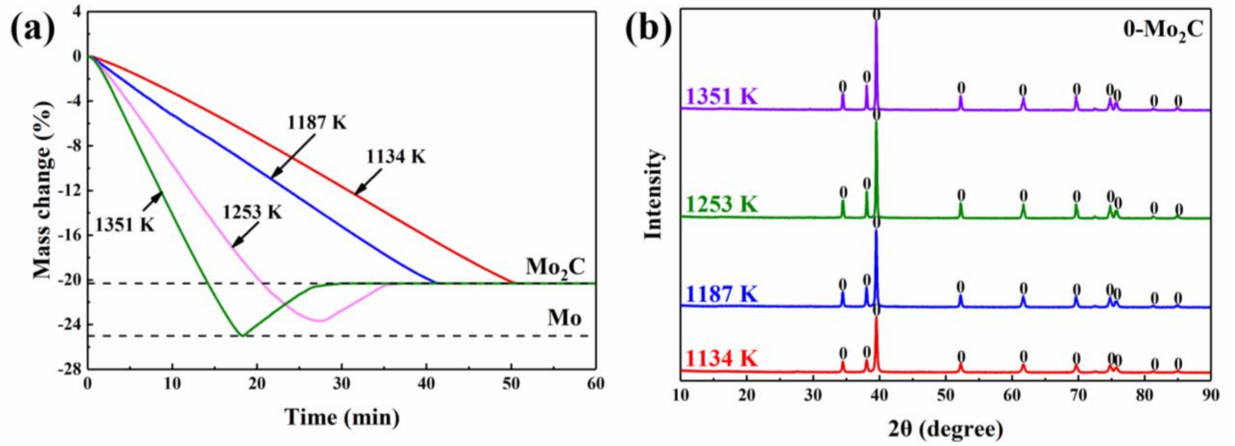

Figure 6. (a) Reduction curves of MoO_2 powders by C_2H_5OH at different Temperatures, (b) XRD patterns of the isothermal products of MoO_2 by C_2H_5OH vapor at different temperatures (equipped with a Cu tube).

4.3 Morphologies of Reduced Samples

Figure 7 shows the morphologies of samples completely reacted at different ramping rates. Morphologies of Mo_2C obtained at different ramping rates are quite different. The final products (Mo_2C particles) obtained at slower ramping rate were composed of both platelet-shaped and small block-shaped particles, but the platelet-shaped particles were in the majority. These dominant particles retained the overall platelet shape of the original MoO_2. However, with the increase of ramping rate, the shape of particles changed dramatically. Some cracks appeared in the surface because of the O removal and the surface of the particles became rough. The SEM images of samples completely reacted at different temperatures are shown in Figure 8. The morphologies of Mo_2C obtained at different temperatures were very similar with the final products obtained in no-isothermal reaction. The final products (Mo_2C particles) obtained at 1134 K (Figure 8(a)) consisted of atactic slice particles which was similar to the original MoO_2. With the temperature increasing, the shape of particles changed dramatically and more and more block-shaped particles were produced. As the temperature rised further, the formation of both spherically shaped and irregularly shaped particles occurred, and finally those particles became dominant. Especially at 1351 K (Figure 8(d)), the obtained Mo_2C were composed of small spherical sub-particles, but these sub-particles began sintering.

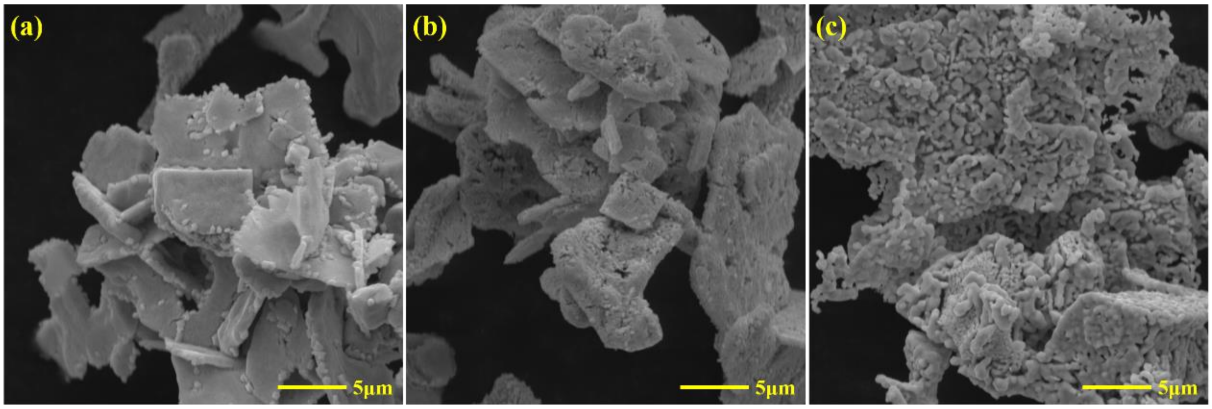

Figure 7. SEM images of samples completely reduced and carbonized at three different ramping rates: (a) 3 K/min, (b) 5 K/min, and (c) 8 K/min.

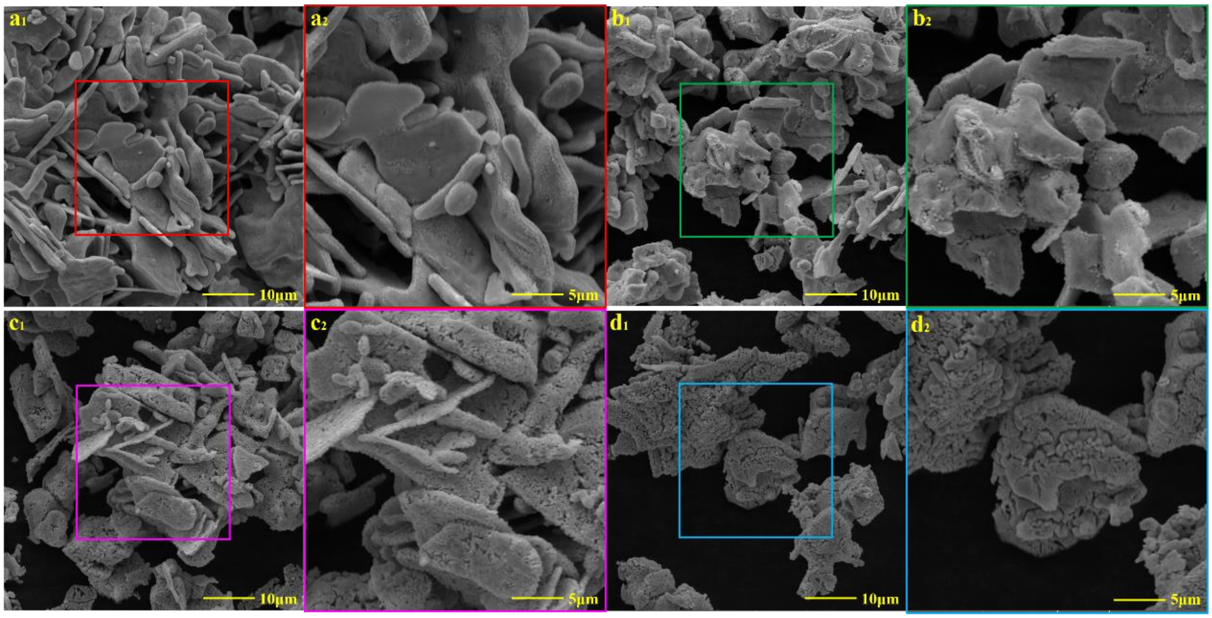

Figure 8. SEM images of samples completely reduced and carbonized at: (a) 1134 K (Mo_2C), (b) 1187 K (Mo_2C), (c) 1253 K (Mo_2C) and (d) 1351 K (Mo_2C).

4.4 Reduction and Carbonization Mechanism

As discussed above, there are two different shapes in the final product (platelet-shaped and block-shaped particles) which was caused by different reaction mechanisms. Two different reaction paths could be found in the process of reactions: pseudomorphic transformation and transformation via CVT (chemical vapor transport). At lower temperatures, the slow reaction rate and low saturated vapor pressure of ethanol decomposition are the main factors for the pseudomorphic transformation mechanism. However, the reduction mechanism, at higher temperatures, should obey the CVT mechanism, because the existence of steam component in the molybdenum oxide powders bed has a great influence on the morphology and size of Mo particle [21]. The diverse morphologies of final products will vary with the reaction mechanisms. Those two kinds of reduction mechanisms are also confirmed by a lot of researches [20-24] during the reduction of molybedenum oxides to Mo. The volatile phase ($MoO_2(OH)_2$) is the main medium of CVT whose formation is depended on the local partial pressure of H_2O during reduction. The amount of the $MoO_2(OH)_2$ increases result from the fast rate of transaction and higher humidity (a lot of water vapor was formed in a short time compared with lower temperatures).

5. Conclusions

This work reported the pyrometallurgical reduction behavior of MoO_2 in Ar-C_2H_5OH atmosphere. Based on the thermodynamic and experimental results, the major conclusions are as follows:

1) The reduction and carbonization routes were obtained: the final product of Mo_2C was formed in one step at a lower temperature; while at high temperatures, MoO_2 was first reduced to Mo and then carbonized to Mo_2C.

2) It was found that the reduction mechanisms were quite different at different temperatures: the pseudomorphic transformation mechanism dominated the reaction at low temperatures, but at high temperatures, the reduction mechanism obeyed the CVT, which was beneficial for grain refining of final products.

Acknowledgements

Thanks are given to the financial supports from the Fundamental and Frontier Research Project of Chongqing (cstc2017jcyjAX0322), the Venture & Innovation Support Program for Chongqing Overseas Returnees (cx2018055), and Young Elite Scientists Sponsorship Program by CAST (2018QNRC001).

References

1. Louis E. Toth, *Transition metal carbides and nitrides* (New York, NY: Academic Press, 1971), 1-26.
2. S. Ted Oyama, The Chemistry of Transition Metal Carbides and Nitrides (London, LON: Blackie Academic & Professional, 1996), 1-27.
3. S. Lia, J.S. Leea, T. Hyeonb and K. Suslickb, “Catalytic hydrodenitrogenation of indole over molybdenum nitride and carbides with different structures”, *Applied Catalysis A: General*, 184 (1999), 1-9.
4. K.R. McCrea, J.W. Logan, T.L. Tarbuck and M.E. Bussell, “Thiophene Hydrodesulfurization over Alumina-Supported Molybdenum Carbide and Nitride Catalysts: Effect of Mo Loading and Phase”, *Journal of Catalysis*, 171 (1997) 255-267.
5. B. Dhandapani, T.S. Clair and S.T. Oyama, “Simultaneous hydrodesulfurization, hydrodeoxygenation, and hydrogenation with molybdenum carbide”, *Applied Catalysis A: General*, 168 (1998) 219-228.
6. S. Liu, H. Wang, K.J. Smith and C.S. Kim, “Hydrodeoxygenation of 2-Methoxyphenol over Ru, Pd, and Mo_2C Catalysts Supported on Carbon”, *Energy & Fuel*, 31 (2017) 6378-6388.
7. J.G. Choi, L. Thompson and J.R. Brenner, “Pyridine Hydrodenitrogenation over Molybdenum Carbide Catalysts”, *Journal of Catalysis*, 154 (1995) 33–40.
8. T. Christofoletti, J.M. Assaf and E.M. Assaf, “Methane steam reforming on supported and

non-supported molybdenum carbides", *Chemical Engineering Journal*, 106 (2005) 97-103.

9. C. Liang, Y. Pinliang and C. Li, "Nanostructured β-Mo_2C Prepared by Carbothermal Hydrogen Reduction on Ultrahigh Surface Area Carbon Material", *Chemistry of Materials*, 14 (2002) 3148-3151.
10. T.C. Xiao, A.P.E. York, H. Al-Megren, C.V. Williams, H.T. Wang and M.L.H. Green, "Preparation and Characterisation of Bimetallic Cobalt and Molybdenum Carbides", *Journal of Catalysis*, 202 (2001) 100-109.
11. T. Xiao, A.P.E. York, K.S. Coleman, J.B. Claridge, J. Sloan, J. Charnock and M.L.H. Green, "Effect of carburising agent on the structure of molybdenum carbides", *Journal of Materials Chemistry*, 11 (2001) 3094-3098.
12. J. Dang, G. Zhang, L. Wang and K. Chou, "Study on Reduction of MoO_2 Powders with CO to Produce Mo_2C", *Journal of the American Chemical Society*, 99 (2016) 819-824.
13. T.Hyeon, M. Fang and K.S. Suslick, "Nanostructured Molybdenum Carbide: Sonochemical Synthesis and Catalytic Properties", *Journal of the American Chemical Society*, 118 (1996) 5492-5493.
14. J.A. Nelson and M.J. Wagner, "High Surface Area Mo_2C and WC Prepared by Alkalide Reduction", *Chemistry of Materials*, 14 (2002) 1639-1642.
15. M. Patel and J. Subrahmanyam, "Synthesis of nanocrystalline molybdenum carbide (Mo_2C) by solution route", *Materials Research Bulletin*, 43 (2008) 2036-2041.
16. H. Preissa, L.M. Bergerb and D. Schultzec, "Studies on the Carbothermal Preparation of Titanium Carbide from Different Gel Precursors", *Journal of the European Ceramic Society*, 19 (1999) 195-206.
17. A. Geng and G.J. Liu, "Preparation of ultramicro molybdenum carbide powders and study on wear properties of their coating", *Rare Metals*, 30 (2011) 262–266.
18. J. Dang, G.H. Zhang and K.C. Chou, "Study on kinetics of hydrogen reduction of MoO_2", *International Journal of Refractory Metals and Hard Materials*, 41 (2013) 356-362.
19. F. Korkmaz, S. Cetinkaya and S. Eroglu, "Thermodynamic Analysis and Reduction of Bismuth Oxide by Ethanol", *Metallurgical and Materials Transactions B: Process Metallurgy and Materials Processing Science*, 47 (2016) 2378-2385.
20. Z. Lv, J. Dang, Y. Wu, X. Lv and S. Zhang, "Preparation of Mo_2C by reduction and carbonization of MoO_2 with CH_3OH", *Journal of Materials Science*, 53 (2018) 10059-10070.
21. J. Dang, G.H. Zhang and K.C. Chou, "A Morphological Study of the Reduction of MoO_2 by Hydrogen", *High Temperature Materials and Processes*, 34 (2015) 417-424.
22. W.V. Schulmeyer and H.M. Ortner, "Mechanisms of the hydrogen reduction of molybdenum oxides", *International Journal of Refractory Metals and Hard Materials*, 20 (2002) 261-269.
23. Y. Wu, J. Dang, Z. Lv and R. Zhang, "The preparation of tungsten carbides and tungsten powders by reaction of tungsten trioxide with methanol", *International Journal of Refractory Metals and Hard Materials*, 76 (2018) 99-107.
24. J. Dang, K.C. Chou, X.J. Hu and G.H Zhang, "Reduction Kinetics of Metal Oxides by Hydrogen", *steel research international*, 84 (2013) 526-533.